DYNAMICS OF GAS BUBBLE GROWTH IN OIL-REFRIGERANT MIXTURES UNDER ISOTHERMAL DECOMPRESSION

João Paulo Dias, jpdias@polo.ufsc.br
Jader R. Barbosa Jr., jrb@polo.ufsc.br
Alvaro T. Prata, prata@polo.ufsc.br
Department of Mechanical Engineering, Federal University of Santa Catarina, Florianópolis, Brazil

Abstract. *This paper proposes a numerical model to predict the growth of gaseous refrigerant bubbles in oil-refrigerant mixtures with high contents of oil subjected to isothermal decompression. The model considers an Elementary Cell (EC) in which a spherical bubble is surrounded by a concentric and spherical liquid layer containing a limited amount of dissolved liquid refrigerant. The pressure reduction in the EC generates a concentration gradient at the bubble interface and the refrigerant is transported to the bubble by molecular diffusion. After a sufficiently long period of time, the concentration gradient in the liquid layer and the bubble internal pressure reach equilibrium and the bubble stops growing, having attained its stable radius. The equations of momentum and chemical species conservation for the liquid layer, and the mass balance at the bubble interface are solved via a coupled finite difference procedure to determine the bubble internal pressure, the refrigerant radial concentration distribution and the bubble growth rate. Numerical results obtained for a mixture of ISO VG10 ester oil and refrigerant HFC-134a showed that bubble growth dynamics depends on model parameters like the initial bubble radius, initial refrigerant concentration in the liquid layer, decompression rate and EC temperature. Despite its simplicity, the model showed to be a potential tool to predict bubble growth and foaming which may result from important phenomena occuring inside refrigeration compressors such as lubrication of sliding parts and refrigerant degassing from the oil stored in oil sump during compressor start-up.*

Keywords*: Refrigeration compressor, oil-refrigerant mixtures, bubble growth, micro-scale model, numerical modeling*

1. INTRODUCTION

The interaction between the lubricant oil is a key aspect in the refrigeration hermetic compressor performance and reliability. Its importance stems from the fact that the oil stored in the compressor sump is kept in direct contact with the gas refrigerant inside the shell. The refrigerant usually has a significant solubility in the oil, which depends on pressure and temperature, and the phase equilibrium is generally attained by means of refrigerant gas absorption and/or release from the mixture in some regions inside the compressor. Especially regarding the gas release, it is caused primarily by the pressure reduction during the compressor start-up, but also due to the pressure reduction due to fluid friction as the saturated lubricant flows through the compressor channels. As a result of the decompression, small gas bubbles are formed which, in turn, change the lubricant properties. If the pressure reduction is fast enough, bubble nucleation is so intense that foam is formed (Becerra, 2003). It has been argued that this can affect the compressor performance parameters, such as the energy consumption, the volumetric efficiency, as well as issues related to noise and wear.

It is well accepted that gas evolution and foam formation in oil-refrigerant mixtures can affect the compressor tribological characteristics (Yanagisawa *et al.*, 1991). Although the first studies concerning the lubrication of the compressor sliding parts neglected the presence of refrigerant dissolved in the oil (Prata *et al*, 2000.; Rigola *et al.*, 2003; Cho and Moon, 2005; Couto, 2006), they had undoubtedly set the foundations for the more recent lubrication models class that considered the effect of a lubricant mixture composed of refrigerant and oil. Among these studies, Grando *et al.* (2006a) proposed simplified lubrication models for journal bearings considering the interaction between the oil and the refrigerant and the existence of a gas/liquid two-phase flow in the lubricant film. Grando *et al.* (2006b) extended their previous model to the piston dynamics analysis for small reciprocating compressors. Their results indicated an increase of friction losses followed by a reduction in load capacity due the presence of gaseous refrigerant dispersed in the lubricant film.

The sometimes complex fluid flow behavior of oil-refrigerant mixtures poses an additional difficulty to the development of more sophisticated lubrication models. Visual experiments of oil rich mixtures flowing through long small diameter tubes carried out by Lacerda *et al.* (2000) and Castro *et al.* (2004) pointed out the existence of bubbly two-phase flow preceded by a significant region of metastable liquid flow. After nucleation, as the pressure gradient departs from the constant value associated with single-phase flow and increases due to refrigerant outgassing, more bubbles are generated and become very closely spaced giving rise to a foamy structure. In the light of these findings, equilibrium models for oil-refrigerant two-phase flow were proposed by Grando and Prata (2003) and Dias and Gasche (2006), who modeled the homogeneous equilibrium two-phase bubbly and foam flow, and by Barbosa *et al.* (2004) and Castro *et al.* (2009) who correlated the two-phase frictional pressure drop. Without empirically-based corrections, the homogeneous equilibrium models showed some large discrepancies with respect to the experimental data of Lacerda *et al.* (2000) and Castro *et al.* (2004), indicating that a non-equilibrium analysis of oil-refrigerant two-phase flow is necessary.

Non-equilibrium models are based on existence of pressure, temperature or chemical potential differences between the gas and the liquid phases. For dispersed systems such as two-phase bubbly and foam flows, non-equilibrium models generally also take into account nucleation and growth of individual gas bubbles immersed in the liquid phase. These models have been widely employed to describe the growth of bubble aggregations and foam expansion in polymers and viscoelastic fluids (Amon and Denson, 1984; Arefmanesh and Advani, 1991; Arefmanesh *et al.*, 1992; Joshi *et al.* 1998) and in magmatic melts (Proussevitch *et al.*, 1993; Proussevitch and Sahagian, 1996).

Despite the significant number of papers in related fields, the physical mechanisms that govern bubble growth in oil-refrigerant mixtures have never been studied from their first principles, so this is the main contribution of the present paper. A numerical model to predict the growth of gas bubbles subjected to isothermal decompression based on the Amon and Denson (1984) and Proussevitch *et al.* (1993) models is proposed in which the transient transport of refrigerant into the bubble is driven by molecular diffusion. The model considers an Elementary Cell (EC) formed by a spherical gas bubble surrounded by a concentric liquid layer with a limited amount of dissolved refrigerant. As the pressure reduces in the liquid layer, a concentration gradient at the expanding bubble interface induces a refrigerant mass flux into the bubble. After a sufficiently long period, the concentration gradient at the bubble interface vanishes, the bubble internal pressure reaches equilibrium and the bubble stops growing, having attained its final equilibrium radius. The equations of conservation of momentum and chemical species for the liquid layer are solved together with the bubble interfacial mass balance via a coupled finite difference procedure to determine the bubble internal pressure, the refrigerant concentration distribution along the liquid layer and the bubble growth rate. It will be demonstrated quantitatively that, for a mixture of ISO VG10 polyolester lubricant oil and refrigerant HFC-134a, the bubble growth process is characterized by three distinct periods. The first period is one of slow rate of growth (controlled by the combined effects of surface tension and normal viscous stresses), the second period is that in which the bubble reaches it maximum radius (diffusion controlled growth), and the third period is characterized by a vanishing concentration gradient in the liquid layer, when the bubble reaches its stable radius. In general terms, the numerical model results showed that bubble growth dynamics depends on the initial bubble and liquid layer radii, the initial refrigerant concentration in the liquid layer, the decompression rate and the elementary cell temperature.

2. MATHEMATICAL MODELLING

Figure 1 shows the schematic diagram of the proposed physical model. It considers an EC in which a spherical bubble is surrounded by a concentric and spherical liquid layer with a limited amount of dissolved liquid refrigerant. At $t=0$ the bubble and the liquid layer initial radii are R_0 and S_0, and the refrigerant concentration in the liquid layer is uniform ($w_{r,0}$). This initial condition is one of mechanical and chemical equilibrium between the gas and the liquid, which is at a pressure $p_{L,0}$. The bubble growth process is initiated when the pressure in the liquid layer is reduced according to a prescribed function $p_L(t)$. As the liquid pressure is reduced, the interfacial refrigerant concentration decreases and a refrigerant concentration gradient in the liquid layer drives the flux of refrigerant into the bubble, increasing its size. At the same time, the liquid layer radius $S(t)$ is allowed to expand together with the bubble, since no constraint is imposed at the outer surface of the liquid layer. It is worth mentioning that thermodynamic equilibrium is assumed at liquid-gas interface, and that the interfacial solubility, w_{sat}, is calculated as a function of the EC temperature and of the bubble internal pressure $p_G(t)$. After a sufficiently long period ($t\rightarrow\infty$) the total amount of refrigerant initially present in the liquid layer evaporates into the bubble, which eventually reaches its final (stable) radius, R_F, and its final internal pressure $p_{G,F}$.

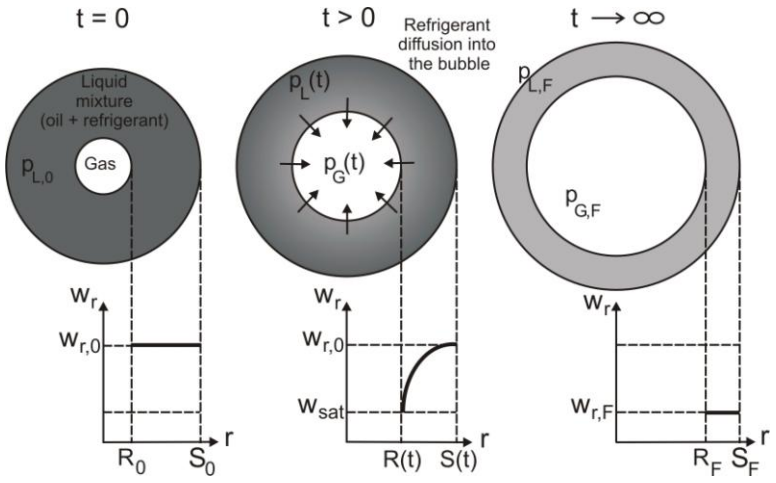

Figure 1. Schematic representation of bubble growth dynamics of an oil-refrigerant mixture.

The mathematical modeling adopts the following assumptions: (i) the bubble and liquid layer are perfectly spherical and the origin of the coordinated axes is placed in the center of the bubble; (ii) the gas phase is composed only by vapour refrigerant and liquid phase is an ideal solution of oil and liquid refrigerant; (iii) the fluids are newtonian; (iv) the temperature gradients in the EC are negligible; (v) the pressures of the bubble and liquid layer are uniform; (vi) the refrigerant mass fraction at the bubble interface is the saturation concentration (solubility) corresponding to the bubble pressure and EC temperature; (vii) the decompression rate imposed in the liquid phase is supposed to be uniform.

2.1. Momentum conservation in the liquid layer

The transient momentum transfer in the liquid layer, in terms of the liquid layer and gas bubble pressure, can be expressed by (Proussevitch *et al.*, 1993),

$$p_G = p_L + \frac{2\sigma}{R} - 4R^2\dot{R}\int_{\zeta(R)}^{\zeta(S)} \mu_L(\zeta)\, d\zeta \tag{1}$$

where σ is the surface tension, R and $\dot{R}$ are the instantaneous radius and its time derivative that represents the bubble growth rate, μ_L is the liquid phase dynamic viscosity and ζ is the auxiliary coordinate related with the radial coordinate, r , defined as follows,

$$\zeta = \frac{1}{r^3};\ \zeta(R) = \frac{1}{R^3};\ \zeta(S) = \frac{1}{S^3} \tag{2}$$

The terms in Eq. (1) represent the various forces acting on the bubble during the growth process. The term on the left hand side is the driving force for bubble growth, while those on the right are the opposing forces, i.e, the pressure acting in the liquid layer, the resistance caused by the surface tension and the liquid viscous forces due to the interface motion.

2.2. Chemical species conservation in the liquid layer

The refrigerant concentration profile in the liquid layer is calculated solving the chemical species conservation equation, which can be defined in terms of a potential function $\varphi(y,t)$ by (Proussevitch *et al.*, 1993),

$$\frac{\partial}{\partial t}\varphi(y,t) = 9D\left(y + R^3\right)^{4/3}\frac{\partial^2}{\partial y^2}\varphi(y,t) \tag{3}$$

where D is the refrigerant mass diffusivity in the liquid mixture, $y = r^3 - R^3(t)$ is a transformation for the radial coordinate that takes into account the movement of bubble interface. The potential function is defined as,

$$\frac{\partial}{\partial t}\varphi(y,t) = w_r(y,t) - w_{r,0} \tag{4}$$

where $w_r(y,t)$ is the refrigerant concentration profile. Equation (3) requires initial and boundary conditions defined as,

$$\varphi(y,0) = 0;\quad \varphi\left(S^3 - R^3, t\right) = 0;\quad \left.\frac{\partial\varphi}{\partial y}\right|_{y=0} = w_{sat} - w_{r,0} \tag{5}$$

The boundary conditions specified in Eq. (5) refer to the uniform refrigerant concentration in the liquid layer at $t=0$, the absence of mass flux through the liquid layer external surface and that the liquid-vapor interface is at thermodynamic equilibrium at the bubble internal pressure and EC temperature.

2.3. Bubble mass balance

The model assumes that molecular diffusion is the principal mechanism by which refrigerant is transported across the interface between the liquid layer and the bubble. Thus, the mass balance in the bubble is given by,

$$\frac{d}{dt}\left(R^3\rho_G\right) = 3R^2\left(\rho_L D\frac{\partial w_r}{\partial r}\right)_{r=R} \tag{6}$$

Expanding the left hand side of Eq. (6) and applying the same transformations used in Eq. (3), the relationship to calculate bubble growth rate results in,

$$\dot{R} = \frac{dR}{dt} = \frac{3R^2}{\rho_G}\left(\rho_L D\frac{\partial^2\varphi}{\partial y^2}\right)_{y=0} - \frac{R}{3\rho_G}\frac{d\rho_G}{dt} \tag{7}$$

2.4. Closure relationships

Equations (1), (3) and (7) are the governing equations of the problem which allow calculation of the gas pressure inside the bubble, the radial refrigerant concentration profile in the liquid layer and the bubble growth rate as a function of time. However, some additional relationships are needed to provide closure for the model.

Initial bubble radius: due the interfacial force acting on the bubble at the first instant of growth, a minimum initial radius must be defined. This minimum initial radius can be expressed in terms of the refrigerant vapor pressure, p_{sat}, at the EC temperature by the Young-Laplace relationship as follows,

$$R_0 > \frac{2\sigma}{p_{sat}(T) - p_{L,0}} \tag{8}$$

Final bubble radius: Proussevitch *et al.* (1993) suggested the use of a total refrigerant mass balance between the initial and final instants of bubble growth to estimate $R(t\to\infty)$ in terms of the liquid and gas phase densities, ρ_L and ρ_G,

$$\left(\rho_G R^3\right)_{t\to\infty} - \left(\rho_G R^3\right)_{t=0} = \left(S_0^3 - R_0^3\right)\left[\left(\rho_L w_r\right)_{t=0} - \left(\rho_L w_{sat}\right)_{t\to\infty}\right] \tag{9}$$

Instantaneous liquid layer radius: as the EC is free to expand, the liquid layer radius can be calculated by solving the following integral relationship for the instantaneous mass of liquid in the liquid layer, $M_L(t)$,

$$M_L(t) = 4\pi\int_{R(t)}^{S(t)} \rho_L(r,t)\, r^2 dr \tag{10}$$

3. NUMERICAL SOLUTION PROCEDURE

A convenient way to solve the coupled non-linear system formed by Eqs (1), (3) and (7) involves the normalization of the variables to make the computational implementation task much easier. Thus, the normalized governing equations are:

$$\hat{p}_G = \hat{p}_L + \frac{Y_3}{\dot{\hat{R}}} + Y_1 Y_2 \hat{R}^2\dot{\hat{R}}\int_0^1 \frac{\mu_L}{\left(\hat{y} + Y_1\hat{R}^3\right)} dy \tag{11}$$

$$\frac{\partial\hat{\varphi}}{\partial\hat{t}} = 9\hat{D}Y_1^{2/3}\left(\hat{y} + Y_1\hat{R}^3\right)^{4/3}\frac{\partial^2\hat{\varphi}}{\partial\hat{y}^2} \tag{12}$$

$$\hat{\varphi}(\hat{y},0) = 0\,; \quad \varphi(1,\hat{t}) = 0\,; \quad \left.\frac{\partial\hat{\varphi}}{\partial\hat{y}}\right|_{\hat{y}=0} = w_{sat} - w_{r,0} \tag{13}$$

$$\dot{\hat{R}} = \frac{d\hat{R}}{d\hat{t}} = \frac{3\hat{R}^2}{\hat{\rho}_G}Y_1\left(\hat{\rho}_L\hat{D}\frac{\partial^2\hat{\varphi}}{\partial\hat{y}^2}\right)_{\hat{y}=0} - \frac{\hat{R}}{3\hat{\rho}_G}\frac{d\hat{\rho}_G}{d\hat{t}} \tag{14}$$

whose the normalized parameters are defined as,

$$\hat{t}=\frac{D_0}{R_0^2};\quad \hat{y}=\frac{y}{S_0^3-R_0^3};\quad \hat{\varphi}=\frac{\varphi}{S_0^3-R_0^3};\quad \hat{p}=\frac{p}{p_{L,0}};\quad \hat{R}=\frac{R}{R_0};\quad \dot{\hat{R}}=\frac{d\hat{R}}{d\hat{t}}=\dot{R}\frac{R_0}{D_0};\quad \hat{D}=\frac{D}{D_0} \tag{15}$$

$$\hat{\rho}=\frac{\rho}{\rho_{G,0}};\quad \mu_{L,0}=\frac{\mu_L}{\mu_{L,0}};\quad \hat{\sigma}=\frac{\sigma}{\sigma_0};\quad Y_1=\frac{R_0^3}{S_0^3-R_0^3};\quad Y_2=\frac{4\mu_{L,0}D_0}{p_{L,0}R_0^2};\quad Y_3=\frac{2\sigma_0}{R_0 p_{L,0}} \tag{16}$$

where the subscript "0" denotes the initial condition. For the solution of Eq. (12), with the boundary conditions presented in Eq. (13), a finite difference-based procedure was used. To accelerate the convergence, another coordinate transformation recommended by Anderson *et al.* (1984) refines the computational grid only in the region near the bubble interface. This coordinate transformation is defined as follows,

$$\hat{y}(y^*)=\beta+1-(\beta-1)\left(\frac{\beta+1}{\beta-1}\right)^{1-y^*}\left[1+\left(\frac{\beta+1}{\beta-1}\right)^{1-y^*}\right]^{-1} \tag{17}$$

$$\frac{\partial\hat{\varphi}}{\partial\hat{y}}=\frac{\partial\hat{\varphi}}{\partial y^*}\frac{dy^*}{d\hat{y}};\quad \frac{\partial^2\hat{\varphi}}{\partial\hat{y}^2}=\frac{\partial\hat{\varphi}}{\partial y^*}\frac{d^2y^*}{d\hat{y}^2}+\frac{\partial^2\hat{\varphi}}{\partial y^{*2}}\left(\frac{dy^*}{d\hat{y}}\right)^2 \tag{18}$$

$$\frac{dy^*}{d\hat{y}}=\frac{2\beta}{\left[\beta^2-(1-\hat{y})^2\right]\ln\left(\frac{\beta+1}{\beta-1}\right)};\quad \frac{d^2y^*}{d\hat{y}^2}=\frac{4\beta(\hat{y}-1)}{\left[\beta^2-(1-\hat{y})^2\right]^2\ln\left(\frac{\beta+1}{\beta-1}\right)} \tag{19}$$

in which $1 < \beta < \infty$ is the clustering parameter. The gridding near the interface becomes finer as this parameter approaches unity. The model considered an oil-refrigerant mixture composed by a polyolester type oil (ISO VG10) and refrigerant HFC-134a. Oil and refrigerant thermophysical properties were provided, respectively, by Dias and Gasche (2006) and McLinden *et al.* (1998). A flowchart of the numerical procedure is shown in Fig. 2.

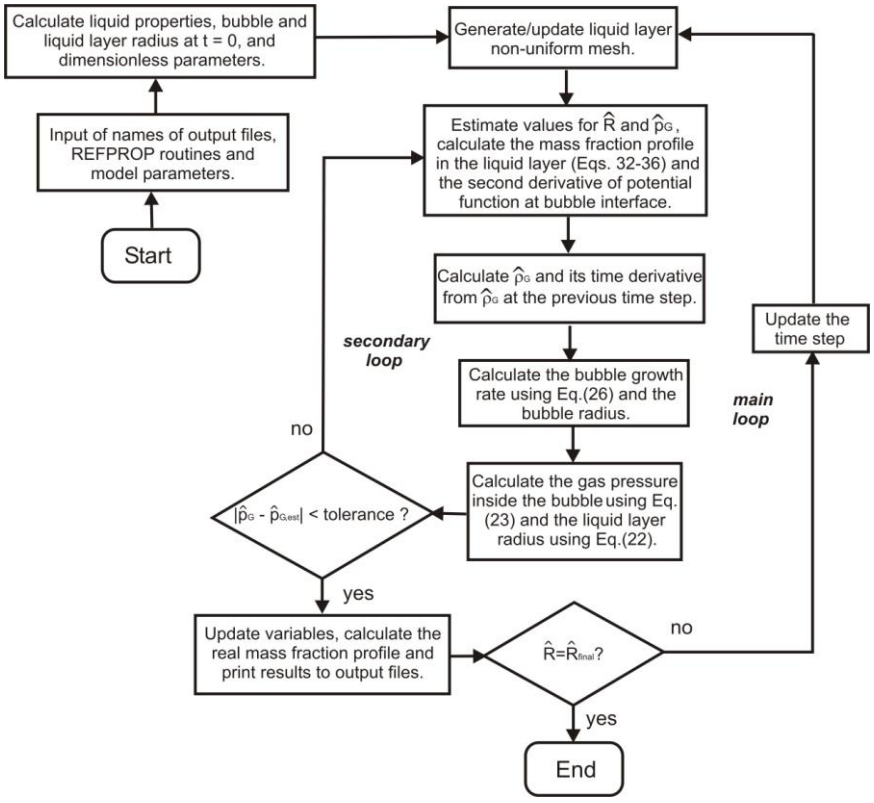

Figure 2. Flowchart of the numerical procedure for the solution of the bubble growth in oil-refrigerant mixtures.

4. RESULTS AND DISCUSSION

A total number of 16 numerical simulations were executed to analyze the model response under different growth conditions. Table 1 shows all cases simulated in the present work, listing the main model inlet and outlet parameters. It is worth mentioning that all numerical results were obtained for a spatial computational grid with 51 nodes in the liquid layer region, time step of 10 μs, and tolerance for the secondary and main loops of 10^{-6} and 99% of the calculated bubble final radius, respectively.

Table 1. Main parameters and results of the simulations realized with the present model.

Simulation	**Parameters**						**Results**			
	S_0 [mm]	R_0 [mm]	$p_{L,0}$ [kPa]	dp_L/dt [kPa/s]	T [^{o}C]	$w_{r,0}$ [%]	$t_{decomp.}$ [s]	t_{final} [s]	R_{final} [mm]	S_{final} [mm]
1	1.00	10^{-2}	100.0	-100.0	60.0	5.0	0.90	1.65	4.99	5.17
2	1.00	10^{-2}	90.0	-100.0	80.0	1.0	0.85	3.96	3.70	3.79
3	1.00	9.5×10^{-2}	90.0	-100.0	80.0	1.0	0.85	3.84	3.70	3.79
4	1.00	0.5	90.0	-100.0	80.0	1.0	0.85	3.65	3.61	3.72
5	1.00	0.9	90.0	-100.0	80.0	1.0	0.85	1.39	3.06	3.24
6	1.00	10^{-2}	90.0	-100.0	80.0	0.95	0.85	3.84	3.63	3.72
7	1.00	10^{-2}	90.0	-100.0	80.0	3.0	0.85	1.49	5.45	5.55
8	1.00	10^{-2}	90.0	-100.0	80.0	5.0	0.85	1.17	6.54	6.67
9	1.00	10^{-2}	90.0	-100.0	80.0	10.0	0.85	0.97	8.37	8.56
10	1.00	10^{-2}	100.0	-10.0	80.0	5.0	9.00	12.7	5.07	5.48
11	1.00	10^{-2}	100.0	-50.0	80.0	5.0	1.80	2.55	5.05	5.34
12	1.00	10^{-2}	100.0	-100.0	80.0	5.0	0.90	1.66	5.10	5.30
13	1.00	10^{-2}	100.0	-100.0	25.0	5.0	0.90	7.50	4.75	4.91
14	1.00	10^{-2}	100.0	-100.0	35.0	5.0	0.90	5.31	4.83	4.99
15	1.00	10^{-2}	100.0	-100.0	50.0	5.0	0.90	3.48	4.93	5.10
16	1.00	10^{-2}	100.0	-100.0	100.0	5.0	0.90	1.55	5.21	5.43

Figure 3 shows the behavior of the bubble and liquid layer radii for Simulation 1. The model computes the liquid layer growth due to bubble expansion (depressurization). The results point out that the bubble growth process is characterized by three distinct periods. The first period is marked by the slow growth of the bubble and the liquid layer radii, which is generally attributed to the high surface tension at the interface. In this period, the growth is controlled by the surface tension and normal viscous stresses that offer a resistance to growth associated with displacing the body of liquid around the bubble. The next 1.2 seconds, where the growth rate increases until a maximum, marks the second period of bubble growth which is called here effective growth period. This period is diffusion controlled as the excess dissolved refrigerant which existed in the first period has now evaporated into the bubble. The bubble and liquid layer reach stable radii in the third period when the refrigerant concentration gradient inside the liquid layer has nearly extinguished. At the end of the process, the bubble and the liquid layer reach, respectively, around 500 and 5 times their initial radii.

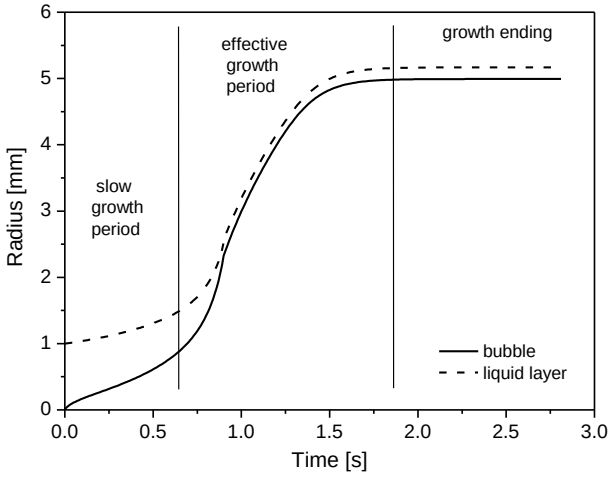

Figure 3. Bubble and liquid layer growth behavior for Simulation 1.

The next result depicted in Fig. 4 analyses the diffusive transport of refrigerant in the liquid layer by comparing the refrigerant concentration profiles in liquid layer at different instants for Simulation 1. Each instant is indicated in the figure as a fraction of the time necessary to bubble reach 99% of its final radius (t_{final}) and the radial coordinate is normalized to facilitate the comparison. Starting from a uniform refrigerant concentration at *t=0*, the first instants after diffusion mechanism has established (until around 30% of t_{final}) indicate almost no change in the concentration profile far from bubble interface whilst high concentration gradients take place near the interface. Then, as bubble growth speed increases, refrigerant solubility at the interface decreases due the gas pressure drop and the gradient at the interface becomes smoother as the refrigerant at the liquid layer periphery starts moving towards the interface, reducing the total amount of refrigerant available in the liquid layer. Finally, after 1.65 s when bubble reaches 99% of its final radius, interfacial concentration reaches the equilibrium with the remaining liquid layer and the bubble stops growing.

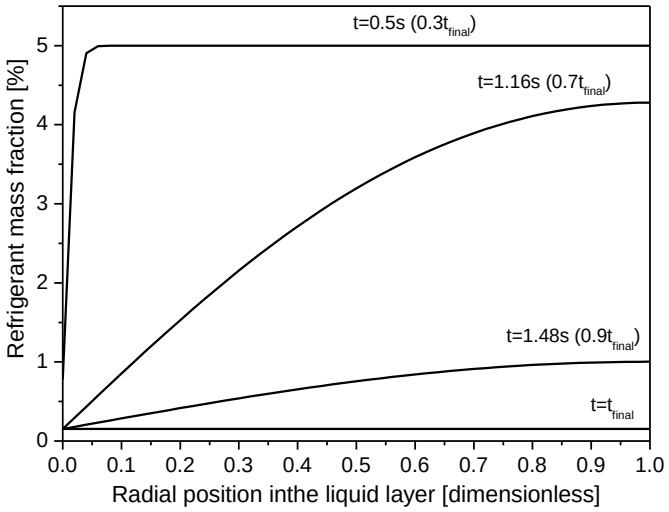

Figure 4. Refrigerant concentration profiles in the liquid layer at different instants for Simulation 1.

Figure 5 shows the effect of variation of the initial bubble radius on the bubble growth behavior. It can be observed that the smaller the initial radius, the longer the slow growth period due the interfacial force at the initial instants when bubble initial radius is too small. Additionally, there is almost no difference between bubble growth curves when initial bubble radius were equal and smaller than 9.5×10^{-2} mm (Simulations 2 and 3). Nevertheless, when initial radius was set at 0.5 and 0.9 mm in Simulations 4 and 5, respectively, the final bubble radius and the time required to reach its stable size decrease because of the reduction in the liquid layer thickness that contains smaller amounts of liquid and volatile material.

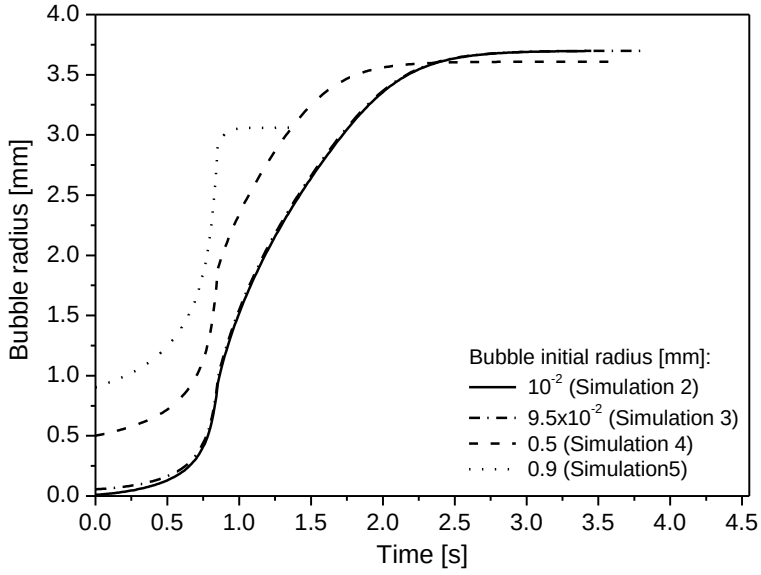

Figure 5. Influence of the initial bubble radius on the bubble growth dynamics.

The effect of variation of initial refrigerant concentration is shown in Fig. 6, which was done with Simulations 6-9 in Table 1. A preliminary analysis of this result led us to conclude that the higher the amount of refrigerant dissolved in the liquid layer initially, the higher bubble final radius. However, the time required to bubble reach its final radius is smaller as the initial refrigerant concentration increases. This occurrence seems to be non-intuitive considering the idea that more refrigerant dissolved in the liquid layer should take more time to flow into the bubble, making it reach the final radius later than the case with less dissolved refrigerant. However, the cases with higher initial refrigerant concentrations presented the steepest slopes in the first 0.8 s. This is a consequence of the high concentration gradients generated in the liquid layer when the concentration increases, once the solubility at the interface remains the same which result in higher mass flux of refrigerant into the bubble.

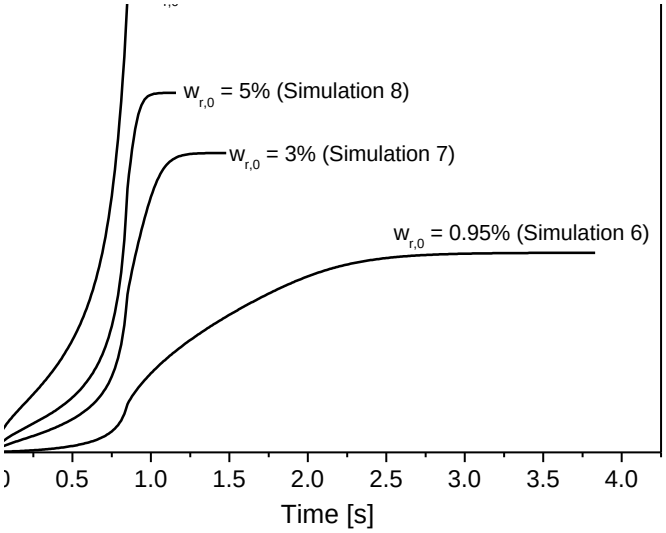

Figure 6. Influence of initial refrigerant mass fraction on bubble growth dynamics.

Differently from the previous models used to study isothermal gas bubble formation in polymers solutions and volcanic magma (Amon and Denson, 1984; Proussevitch *et al.*, 1993), we assumed here a finite decompression rate in the liquid phase from both prescribed initial and final pressure in the liquid layer. This is a convenient approach to deal with oil-refrigerant mixtures since this model can be coupled to existing macroscopic models aiming a more complete characterization of non-equilibrium flow of oil-refrigerant mixtures (Barbosa, 2004). Figure 7 depicts the behavior of bubble growth for Simulations 10-12 considering different liquid phase decompression rates. The plots indicate that as the pressure in the liquid layer is reduced, more time is needed for the bubble to reach its final radius. This behavior occurs because bubble growth driven by gas expansion becomes slower than that due to interfacial refrigerant mass flux as the decompression rate decreases.

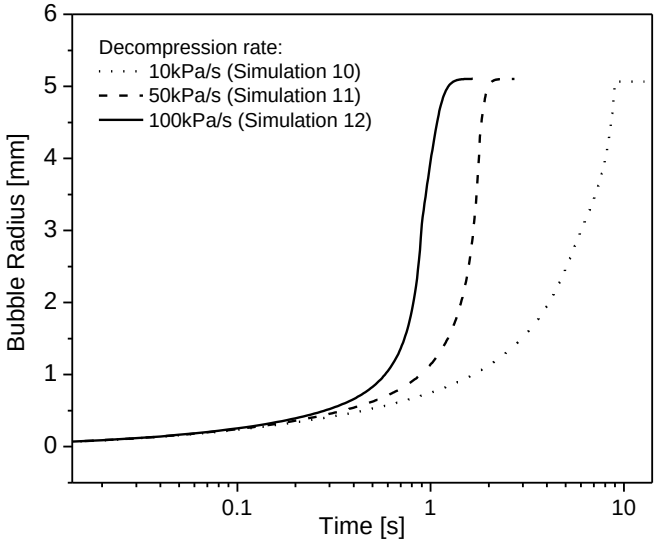

Figure 7. Influence of decompression rate in the liquid phase on bubble growth dynamics.

Figure 8 presents an analysis of the effect of the EC temperature on the bubble radius behavior as a function of time for Simulations 13-16. An increase of the EC temperature reduces the dynamic viscosity and increases the mass diffusivity of the mixture so that the combination of both factors leads to faster bubble growth rates since, as the EC temperature increases, viscous forces that resist to bubble growth are smaller and, at the same time, large mass diffusion coefficients contributes to improving refrigerant mobility inside the liquid layer. Another observation regarding the effect of EC temperature on bubble dynamics is the different final radius reached in each simulation. This occurs because equilibrium concentration at the interface is an inverse function of the EC temperature which results in a higher oversaturation degree in the liquid layer. So, larger contents of refrigerant can flow into the bubble making its final radius higher.

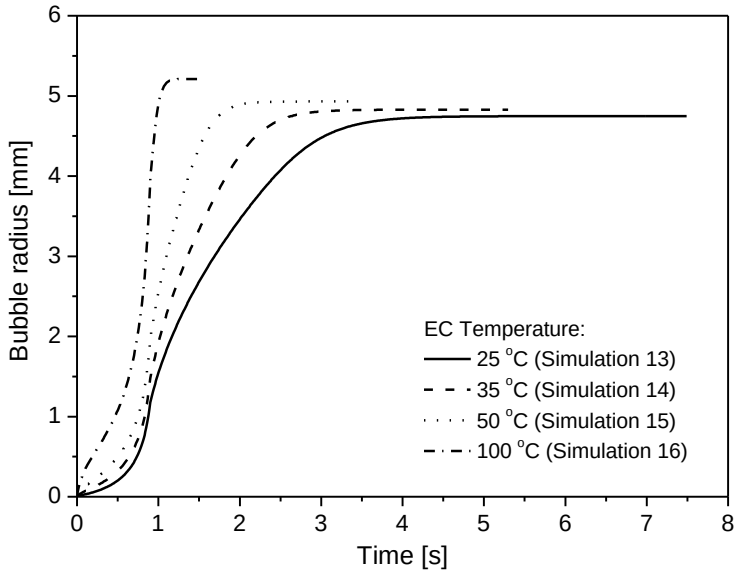

Figure 8. Influence of temperature in the elementary cell on bubble growth dynamics.

5. CONCLUSIONS

This paper presented a transient model of one single gas bubble growing in an oil-refrigerant solution submitted to uniform and isothermal decompression. The model considered a bubble surrounded by a liquid layer containing a limited amount of dissolved refrigerant (Elementary Cell) where the pressure reduction on the liquid phase provokes the imbalance between initial refrigerant concentration in the liquid layer and the equilibrium concentration at the interface. This phenomenon initiates the mass diffusion process of refrigerant from the liquid layer to the bubble resulting bubble expansion. After a long period, the bubble tends to reach a stable radius as both decompression and the amount of refrigerant in the liquid layer are extinguished. The coupled and non-linear set of governing equations of the problem where solved numerically to calculate model variables such as bubble internal pressure, bubble growth rate and the refrigerant concentration profiles in the liquid layer.

The numerical results showed that, in general terms, the bubble growth process presented three distinct periods: the first period of slow growth rate, the second period of rapid bubble expansion followed by the third period of radius stabilization. The refrigerant mass fraction profiles along the liquid layer pointed out higher gradients at the interface region during the initial instants whereas the final instants presented smoother gradients as the amount of refrigerant in the layer runs out. The parametric analysis of the model showed that an increase of the bubble initial radius results in a decrease of the bubble stable radius and of its total growth time. Moreover, the higher the amount of refrigerant initially dissolved in the liquid layer, the smaller the time required to bubble grow completely and the higher bubble stable radius. The evaluation of the influence of decompression rate showed that for longer pressure reduction on the liquid phase, the total growth period tends to increase. The results obtained considering different EC temperatures lead to faster bubble growth and larger stable radius explained by the influence of temperature on viscosity and refrigerant diffusivity on the oil-refrigerant mixture.

6. ACKNOWLEDGEMENTS

The authors thank EMBRACO S.A., FINEP and CNPq for financially supporting this work.

7. REFERENCES

Amon, M. and C. Denson, 1984, "A Study of the Dynamics of Foam Growth: Analysis of the Growth of Closely Spaced Spherical Bubbles", Polymer Engineering and Science, Vol. 24, pp. 1026-1034.

Anderson, D. A., J. C. Tanehill and R. H. Pletcher, 1984, "Computational Fluid Mechanics and Heat Transfer", Hemisphere Publishing Co., Washington.

Arefmanesh, A. and Advani, S. G, 1991, "Diffusion-Induced Growth of a Gas Bubble in a Viscoelastic Fluid", Rheologica Acta, Vol. 30, pp. 274-283.

Arefmanesh, A., Advani, S.G., Michaelides, E.E., 1992, "An Accurate Numerical Solution for Mass Diffusion-Induced Bubble Growth in Viscous Liquids Containing Limited Dissolved Gas", International Journal of Heat and Mass Transfer, Vol. 35, pp. 1711-1722.

Barbosa Jr., J.R., 2004, "Operações e Escoamento Bifásico de Misturas de Fluido Refrigerante e Óleo Lubrificante Visando o Projeto de Compressores Herméticos", Monografia Concurso Professor Adjunto (in Portuguese), Federal University of Santa Catarina.

Barbosa Jr., J.R., Lacerda, V.T. and Prata, A.T., 2004, "Prediction of Pressure Drop in Refrigerant-Lubricant Oil Flows with High Contents of Oil and Refrigerant Outgassing in Small Diameter Tubes", Int. Journal of Refrigeration, Vol. 27, nº 2, pp.129-139.

Becerra, E.C.V., 2003, "Simulação de um Compressor Hermético Alternativo Operando em Regime Transiente", D.Eng. thesis (in Portuguese), PUC-Rio.

Castro, H. O. S., Gasche, J. L. and Conti, W. P., 2004, "Foam Flow of Oil-Refrigerant R134a Mixture in a Small Diameter Tube" Proc. of the 10th Int. Refrigeration and Air Conditioning Conference at Purdue, Purdue, USA.

Castro, H. O. S., Gasche, J. L. and Prata, A. T., 2009, "Pressure Drop Correlation for Oil-Refrigerant R134a Mixture Flashing Flow in a Small Diameter Tube", International Journal of Refrigeration, Vol. 32, pp.421-429.

Cho, J.R. and Moon, S.J., 2003, "A Numerical Analysis of the Interaction Between the Piston Oil Film and the Component Deformation in a Reciprocating Compressor", Tribology International, Vol. 38, pp. 459-468.

Couto, P. R. C., 2007, "Análise de Mancais Radiais Hidrodinâmicos com Aplicação em Compressores Herméticos de Refrigeração", D. Eng. Thesis (in Portuguese), Federal University of Santa Catarina.

Dias, J. P. and Gasche, J. L., 2006, "Computational Simulation of the Oil-R134a Mixture Two-Phase Flow with Foam Formation in a Circular Cross Section Tube", Proc. of ECI Int. Conference on Boiling Heat Transfer, Spoleto, Italy.

Grando, F.P. and Prata, A.T., 2003, "Computational Modeling of Oil-Refrigerant Two-Phase Flow with Foam Formation in Straight Horizontal Pipes", Proc. of the 2nd HEFAT, Zambia.

Grando, F.P., Priest, M. and Prata, A.T., 2006a, "A Two-Phase Flow Approach to Cavitation Modeling in Journal Bearings", Tribology Letters, Vol. 21, n° 3, pp. 233-244.

Grando, F.P., Priest, M. and Prata, A.T., 2006b, "Lubrication in Refrigeration Systems: Numerical Model for Piston Dynamics Considering Oil-Refrigerant Interaction", Proc. of IMechE Part J: Journal of Engineering Tribology, Vol. 220, pp. 245-258.

Joshi, K., Lee, J. G., Shafi, M.A. and Flumerfelt, R.A., 1998, "Prediction of Cellular Structure in Free Expansion of Viscoelastic Media", Journal of Applied Polymer Science, Vol. 67, 1353-1368.

Lacerda. V.T., Prata, A.T. and Fagotti, F., 2000, "Experimental Characterization of Oil-Refrigerant Two-Phase Flow", Proc. of the ASME – Advanced Energy Systems Division, Vol. 40, pp. 101-109.

McLinden, M.O., Klein, S.A., Lemmon, E.W. and Peskin, A.P., (1998) "Thermodynamic and Transport Properties of Refrigerants and Refrigerants Mixtures", NIST Standard Reference Database 23, REFPROP 6.0.

Prata, A.T., Fernandes, J.R.S. and Fagotti, F., 2000, "Dynamic Analysis of Piston Secondary Motion for Small Reciprocating Compressors", Transactions of the ASME – Journal of Tribology, Vol. 122, pp. 752-760.

Proussevitch, A. A., Sahagian, D. L. and Anderson, A. T., 1993, "Dynamics of Diffusive Bubble Growth in Magmas: Isothermal Case", Journal of Geophysical Research, Vol. 98, pp. 22283-22307.

Proussevitch, A. A. and Sahagian, D. L., 1996, "Dynamics of Coupled Diffusive and Decompressive Bubble Growth in Magmatic Systems", Journal of Geophysical Research, Vol. 101, pp. 17447-17455.

Rigola, J., Pérez-Segarra, C.D. and Oliva, A., 2003, "Numerical Simulation of the Leakage Through the Radial Clearance Between Piston and Cylinder in Hermetic Reciprocating Compressors", Proc. of the Int. Conference on Compressor and their Systems, London, UK, pp. 313-321.

Yanagisawa, T., Shimizu, T., Fukuta, M., 1991, "Foaming Characteristics of an Oil-Refrigerant Mixture", International Journal of Refrigeration, Vol. 14, pp. 132-136.

8. RESPONSIBILITY NOTICE

The authors are the only responsible for the printed material included in this paper.